Geometries and Electronic Properties of the Tungsten-Doped Germanium Clusters: WGe_n ($n = 1-17$)

Jin Wang[†,§] and Ju-Guang Han*[,‡]

Department of Chemistry, University of Guelph, Guelph, N1G 2W1, Ontario, Canada, and Department of Chemistry and Biochemistry, Montana State University, Bozeman, Montana 59717

Received: June 10, 2006; In Final Form: September 10, 2006

Geometries associated with relative stabilities, energy gaps, and polarities of W-doped germanium clusters have been investigated systematically by using density functional theory. The threshold size for the endohedral coordination and the critical size of W-encapsulated Ge_n structures emerge as, respectively, $n = 8$ and $n = 12$, while the fullerene-like $W@Ge_n$ clusters appears at $n = 14$. The evaluated relative stabilities in term of the calculated fragmentation energies reveal that the fullerene-like $W@Ge_{14}$ and $W@Ge_{16}$ structures as well as the hexagonal prism WGe_{12} have enhanced stabilities over their neighboring clusters. Furthermore, the calculated polarities of the $W@Ge_n$ reveal that the bicapped tetragonal antiprism WGe_{10} is a polar molecule while the hexagonal prism WGe_{12} is a nonpolar molecule. Moreover, the recorded natural populations show that the charges transfer from the germanium framework to the W atom. Additionally, the WGe_{12} cluster with large highest occupied molecular orbital−lowest unoccupied molecular orbital (HOMO−LUMO) gap, large fragmentation energy, and large binding energy is supposed to be suitable as a building block of assembly cluster material. It should be pointed out that the remarkable features of $W@Ge_n$ clusters above are distinctly different from those of transition metal (TM) doped Ge_n (TM = Cu and Ni) clusters, indicating that the growth pattern of the $TMGe_n$ depends on the kind of doped TM impurity.

I. Introduction

Transition metal doped semiconductor clusters are currently of great interest in that the sized selectivities, tunable gaps, and magnetic properties can lead to novel self-assembly nanoscale optoelectronic materials. Recent theoretical and experimental investigations on the TM-doped germanium clusters indicate that the TM-doped germanium clusters differ from the TM-doped silicon clusters in growth patterns.[1−3] Our previous calculations on the first-row TM-doped germanium clusters indicate that the $TM@Ge_{10}$ (TM = Ni and Cu) have larger relative stabilities as compared to those of other sized $TM@Ge_n$ ($n = 1-9, 11-13$; TM = Ni and Cu) clusters, which is in good agreement with experimental observations of $CoGe_{10}^-$ and theoretical results.[1,4−6] As far as the TM-doped germanium clusters are concerned, no systematic investigations on the different sized TM-doped Ge_n clusters have been investigated in detail until now. Hence, the relative stabilities of the species $TM@Ge_{10}$, $TM@Ge_{12}$, and $TM@Ge_{16}$, the threshold germanium number of the TM-encapsulated caged Ge_n structures, the cagelike or fullerene-like TM-encapsulated Ge_n geometries, the charge-transfer mechanisms, and various growth pattern behaviors of the TM-doped germanium clusters or TM-doped silicon clusters are studied because this remarkable information makes them attractive for cluster-assembled materials. In this paper, the detailed investigations on equilibrium geometries associated with stabilities and energy gaps of the W-doped Ge_n clusters are performed at the UB3LYP/LanL2DZ level.

II. Computational Details

The geometry optimizations of the WGe_n ($n = 1-17$) clusters are carried out by density functional theory (DFT) with the unrestricted B3LYP exchange-correlation potential and effective core potential (ECP) LanL2DZ basis sets.[7,8] The standard LanL2DZ basis sets,[7,8] which provide an effective way to reduce difficulties in calculations of two-electron integrals caused by heavy transition metal atoms, are employed. Moreover, the LanL2DZ basis sets with the scalar relativistic effects considered do not degrade when the transition metal changes from the second- to the third-row transition metal element. In a previous paper, the LanL2DZ basis sets of ECP theory and the B3LYP method were proven to be reliable for predicting the geometries, stabilities, and electronic properties of Ge_n, $TM@Si_n$, and the first-row $TM@Ge_n$ (TM = Ni and Cu) systems.[4,9−13] The calculated results confirmed that the energetic ordering of the competitive isomers for the definite sized $TM@Ge_n$ clusters at the B3LYP/GEN level (LanL2DZ for the TM atom and 6-31G for the Ge_n atoms) is essentially unchanged as compared to the results calculated using the B3LYP/LanL2DZ method. The ECP approach used in the present context subdivides the electronic system of the W atom into a core consisting of the K, L, M, and N shells and a $5s^25p^65d^46s^2$ valence region described by three basis functions of s character and three p and two d basis functions. Likewise, the Ge core comprises the K, L, and the M shells, and two s, as well as two p basis functions, corresponding to the $4s^24p^2$ system, define the valence region. The bond length, averaged atomic binding energy, and lowest harmonic vibrational frequencies of the Ge_2, W_2, and WGe molecules are calculated at the B3LYP/lanL2DZ and B3LYP/

* To whom correspondence should be addressed. E-mail: jghan@ustc.edu.cn. Fax: +86-551-5141078.
† University of Guelph.
‡ Montana State University.
§ On leave from the National Synchrotron Radiation Laboratory, University of Science and Technology of China, Hefei 230026, People's Republic of China.

10.1021/jp0636219 CCC: $33.50
Published on Web 10/28/2006

TABLE 1: Bond Length (*R*, angstrom), Averaged Atomic Binding Energy (E_b/Atom, eV), and the Lowest Harmonic Vibrational Frequency (freq, cm^{-1}) for the Ground State of the Following Molecules

molecule	method	spin	*R*	E_b	freq	electronic state
Ge_2	B3LYP/LanL2DZ	1	2.528	1.172	250.1	$^3\Sigma_g$
	B3LYP/6-31G	1	2.421	1.502	262.7	$^3\Sigma_g$
W_2	B3LYP/LanL2DZ	0	2.039	1.836	410.6	$^3\Sigma_g$
	EXP[a]					$^3\Sigma_g^+$
GeW	B3LYP/LanL2DZ	1	2.325	1.123	287.9	$^3\Delta$
	B3LYP/GEN	1	2.328		299.5	$^3\Delta$

[a] Ref 14.

GEN levels and are listed in Table 1; for further evidences in this paper, the calculated values at the B3LYP/LanL2DZ level are in good agreement with those at the B3LYP/GEN level, which are in good agreement with available experimental and theoretical results,[14] indicating that our calculations are reliable and accurate, which will provide reliable data of the WGe_n ($n = 1-17$) clusters. This examination of equilibrium bond lengths and angles leads to deviations of typically 1−6%. Because of its reliance on pseudopotentials, our study has to be considered as preliminary and qualitative in nature. In this paper, all theoretical calculations are carried out with Gaussian 03 program package;[15] the numerous adsorption sites of the Ge atom and substitution sites of the W impurity on the small-sized Ge_n clusters are investigated, while no stable geometries for the small-sized WGe_n geometries with the W impurity being localized at the center sites were found until $n \geq 8$. Acknowledging the nonzero spin of most of the species investigated, the spin-unrestricted formalism (U) has been applied; the spin triplet state of very small-sized WGe_n clusters ($n \leq 2$) and the spin singlet state of the large-sized WGe_n ($n \geq 3$) clusters are the lowest energy geometries.

III. Results and Discussions

III.A. Equilibrium Structures of WGe_n ($n = 1-9$). The spin triplet state of the $C_{\infty v}$ WGe dimer with an electronic state of $^3\Delta$ is the most stable geometry and ground state, which is similar to the triplet NiGe dimer.[4] The linear $D_{\infty h}$ WGe_2 structure is a stable structure; however, its total energy is higher than that of the closed triangular C_{2v} WGe_2 structure, indicating that its stability is weakened as compared to that of the latter. Furthermore, the total energy of the closed triangular triplet C_{2v} structure is lower than that of the identical singlet structure by 0.54 eV, and the corresponding electronic ground state of WGe_2 is $^3A_2$.

As for the small-sized W-doped Ge_n ($n = 1-3$) clusters, the electronic state of the lowest energy structures also varies from the spin triplet state ($n = 1$ and 2) to the spin singlet state at the size of $n = 3$. Therefore, the spin singlet state is discussed for the large-sized WGe_n ($n \geq 3$) clusters. As seen from the optimized geometries of the WGe_3 clusters, the dominant geometries are the planar and pyramidal structures when the size of the cluster is equal to three. Furthermore, the total energy of the pyramidal 3a structure is lower than that of the planar rhombic 3b structure by 1.92 eV. The interactions between W and Ge atoms in the pyramidal structure are obviously strengthened because the W−Ge bond length (2.39 Å) in the pyramidal 3a structure is shorter than that (2.43 Å) in the rhombic 3b structure. According to the natural bonding orbitals (NBO), the stabilization energy of orbital interactions between the W lone pair NBO and the antibonding W−Ge NBOs in the pyramidal structure are analyzed, and the calculated result is 7.45 kcal/mol. Different from the lowest energy pyramidal WGe_3 3a cluster, previous studies on the first-row TM-doped germanium clusters ($n = 3$) with TM = Cu and Ni indicate that the lowest energy structures are the planar rhombic structure.[4,13] It is worth mentioning that the most stable WGe_3 3a geometry is similar to that of the C_{3v} WSi_3 isomer.[3]

Previous studies[4,13] on the fist-row TM-doped Ge_n (TM = Cu, Ni; $n = 4$ and 5) clusters indicate that the dominant geometries are the TM-capped bent rhombic pyramidal Ge_n structures. For the W-doped Ge_4 clusters, the calculated results show that the W in the most stable WGe_4 cluster participates in bonding with all germanium atoms; a pyramidal W-doped Ge_4 structure is formed after one new germanium atom is capped on the quasi-planar rhombus frame. Furthermore, the most stable W-doped Ge_4 geometry is similar to that of WSi_4 structure.[3] As for the WGe_5 clusters involved, a low-lying high-symmetry W-doped Ge_5 structure is generated after the new germanium atom is absorbed on the quasi-planar rhombus surface. As illustrated in Table 2, the total energy of the high-symmetry C_{4v} 5a structure is lower than that of the nonsymmetrical 5b structure by 0.32 eV. Consequently, the C_{4v} 5a structure is the most stable isomer, showing that the C_{4v} 5a structure keeps the framework that is analogous to the WSi_5 isomer.[3]

The first-row TM (TM = Cu and Ni) doped germanium clusters are the guides.[4,13] The cubic WGe_6 structures, which are based on the rhombic Ge_6 framework, are yielded when $n = 6$. Interestingly, different inserted sites of the W atom in the cubic Ge_6 frame lead to different energetic isomers for the identical sized cluster. As seen from Figure 1, the most stable WGe_6 6a and WGe_7 7a structures are generated after two germanium atoms are symmetrically capped on the pyramidal WGe_4 geometry. It should be pointed out that the calculated total energies reveal that the stability of the cubic WGe_7 7a structure with a 6-fold rhombus is much stronger than that of the tetrahedral pyramidal 7b structure in that the total energy of the 7a isomer is much lower than that of the 7b isomer by 1.04 eV.

The threshold size of the endohedral WGe_n clusters turns out to be $n = 8$. Although some W surface-substituted structures, e.g., tetrahedral pyramidal structures etc., are also found as the stable structures, their total energies are obviously higher than that of the W-encapsulated polyhedral 8c structure. The observed 8c structure, which can be seen as the evidence of the TM-encapsulated germanium framework, is the most stable structure; the W in the 8c isomer, which can be described as the W atom interacting with four germanium atoms directly, localizes at the center site of two pentagons of the germanium framework. This geometry, however, is different from the most stable structures of the first-row TM-doped Ge_n (TM = Cu and Ni) clusters.[4,13]

As far as the WGe_9 clusters are concerned, all optimized stable W-doped germanium clusters have been characterized as the W being sunken into the germanium polyhedron. The most stable 9a isomer, which can be described as the W atom being concave-capped in the slightly distorted C_{4v} Ge_9 isomer, is obtained. As seen from the optimized WGe_9 structures, the W atom of the 9a isomer is surrounded by the germanium frame and the W−Ge bond lengths vary from 2.551 to 2.843 Å. As compared to the small-sized tetrahedral pyramidal WGe_n clusters, the W atom in the stable 9b structure is encapsulated into the tetrahedral pyramidal Ge_9 frame.

III.B. Equilibrium Geometries and Stabilities of the Caged WGe_n ($n = 10-17$). On the basis of the previous investigations on the first-row TM-doped Ge_{10} (TM = Cu, Ni, and Co) clusters,[4−6,13] one confirms that the bicapped tetragonal antiprism

TABLE 2: Geometries and Total Energies of WGe_n (n = 1−17) Clusters[a]

cluster	sym	state	freq (cm^{-1})	R_{W-Ge} (Å)	R_{Ge-Ge} (Å)	E_T (hartree)	ΔE (eV)
WGe	C_v	$^3\Delta$	287.6	2.325		−71.4087609	
WGe_2	C_{2V} (a)	$^3A_2$	141.3	2.405	2.712	−75.2450812	
	D_h (b)	^1B	157.8	2.355		−75.1147725	3.55
WGe_3	C_{3V} (a)	$^1A_1$	96.2	2.39	3.024	−79.0743667	
	C_{2V} (b)	$^1A_1$	72.6	2.425	2.537	−79.0036998	1.92
WGe_4	C_s (a)	$^1A'$	58	2.404	2.603	−82.8518954	
WGe_5	C_{4v} (a)	$^1A_1$	93.4	2.514	2.783	−86.6510549	
	C_1 (b)	^1A	43.1	2.437	2.584	−86.6393112	0.32
WGe_6	C_s (a)	$^1A'$	66.1	2.497	2.556	−90.4400725	
	C_s (b)	$^1A'$	51.8	2.438	2.611	−90.4304657	0.26
	C_s (c)	$^1A'$	56.8	2.492	2.523	−90.4328406	0.2
	C_s (d)	$^1A'$	39.7	2.442	2.675	−90.4268533	0.36
WGe_7	C_1 (a)	^1A	63	2.496	2.626	−94.2361233	
	C_s (b)	$^1A'$	20.8	2.519	2.638	−94.1978984	1.04
	C_1 (c)	^1A	66.3	2.469	2.581	−94.2158083	0.55
WGe_8	C_1 (a)	^1A	26.2	2.499	2.583	−98.0147576	0.85
	C_1 (b)	^1A	38.5	2.611	2.71	−98.0239347	0.6
	C_1 (c)	^1A	4.8	2.517	2.506	−98.0458772	
	C_s (d)	$^1A'$	43.5	2.456	2.594	−98.0055055	1.09
	C_1 (e)	^1A	7.7	2.458	2.561	−98.0299713	0.43
WGe_9	C_1 (a)	^1A	43.4	2.551	2.575	−101.851081	
	C_1 (b)	^1A	36.1	2.504	2.532	−101.8335625	0.48
	C_1 (c)	^1A	37.1	2.524	2.584	−101.8248801	0.71
	C_s (d)	$^1A'$	33.8	2.504	2.628	−101.8202354	0.84
WGe_{10}	C_1 (a)	^1A	36.9	2.507	2.646	−105.6500233	0.05
	C_1 (b)	^1A	27.6	2.531	2.518	−105.6271451	0.68
	C_1 (c)	^1A	37.2	2.486	2.553	−105.6421215	0.27
	C_1 (d)	^1A	17.7	2.478	2.758	−105.6520045	
	C_1 (e)	^1A	25.5	2.474	2.568	−105.6211565	0.84
WGe_{11}	C_2 (a)	^1A	25.7	2.581	2.504	−109.4372329	
	C_1 (b)	^1A	31.8	2.562	2.569	−109.4175496	0.54
	C_1 (c)	^1A	30.6	2.523	2.579	−109.4330856	0.11
	C_1 (d)	^1A	27.2	2.495	2.494	−109.4097178	0.75
WGe_{12}	C_1 (a)	^1A	28.4	2.561	2.493	−113.2143778	0.83
	D_{3d} (b)	$^1A_{1g}$	52.3	2.712	2.569	−113.2450288	
	C_s (c)	$^1A'$	13.1	2.666	2.618	−113.2227588	0.61
	C_s (d)	$^1A'$	20.2	2.622	2.595	−113.2159817	0.79
	C_1 (e)	^1A	18.5	2.516	2.531	−113.1872784	1.57
	C_1 (f)	^1A	16.8	2.578	2.534	−113.2043697	1.11
WGe_{13}	C_1 (a)	^1A	37.7	2.614	2.484	−117.0205729	
	C_1 (b)	^1A	14.4	2.552	2.483	−117.016615	0.11
	C_1 (c)	^1A	19.9	2.659	2.566	−117.0184083	0.06
	C_1 (d)	^1A	35	2.589	2.506	−117.0036815	0.46
	C_1 (e)	^1A	33.5	2.518	2.537	−116.9791363	1.13
WGe_{14}	C_1 (a)	^1A	39.1	2.686	2.481	−120.8201343	
	C_1 (b)	^1A	17.3	2.761	2.447	−120.8032555	0.46
	C_1 (c)	^1A	31.2	2.669	2.478	−120.8020155	0.49
	C_1 (d)	^1A	31.2	2.569	2.558	−120.8005041	0.53
	C_1 (e)	^1A	21.2	2.658	2.529	−120.7871845	0.9
	C_1 (f)	^1A	13.8	2.612	2.517	−120.7644481	1.52
WGe_{15}	C_1 (a)	^1A	12.9	2.762	2.453	−124.5907262	0.27
	C_s (b)	$^1A'$	20.1	2.821	2.475	−124.5910758	0.26
	C_1 (c)	^1A	39.1	2.661	2.429	−124.597338	0.09
	C_1 (d)	^1A	40.4	2.623	2.454	−124.6006317	
	C_1 (e)	^1A	16.1	2.56	2.485	−124.5508073	1.35
	C_1 (f)	^1A	16.2	2.672	2.499	−124.5835868	0.46
WGe_{16}	C_1 (a)	^1A	7.2	2.814	2.449	−128.3943823	
	C_1 (b)	^1A	33.5	2.681	2.457	−128.3495717	1.22
	C_1 (c)	^1A	36.1	2.748	2.476	−128.3703424	0.65
WGe_{17}	C_1 (a)	^1A	31.3	2.674	2.457	−132.1528756	
	C_1 (b)	^1A	36.8	2.727	2.465	−132.1474679	0.15

[a] Sym means point-group symmetry, freq represents the lowest vibrational frequency, R_{w-Ge} and R_{Ge-Ge} denote the shortest bond lengths of W−Ge and Ge−Ge, respectively, E_T denotes the total energies of different WGe_n conformers, and ΔE denotes the relative energy of every conformer and the lowest energy identical size cluster.

structure with the TM being totally encapsulated into the caged Ge_{10} frame is the lowest energy structure and has nearly equivalent bond lengths with surrounded germanium atoms. In the case of WGe_{10} isomers, considering of the bicapped tetragonal antiprism structure, the optimized 10d geometry with unsaturated dangling bonds of germanium atoms is seriously distorted. As can be seen from the findings related to the

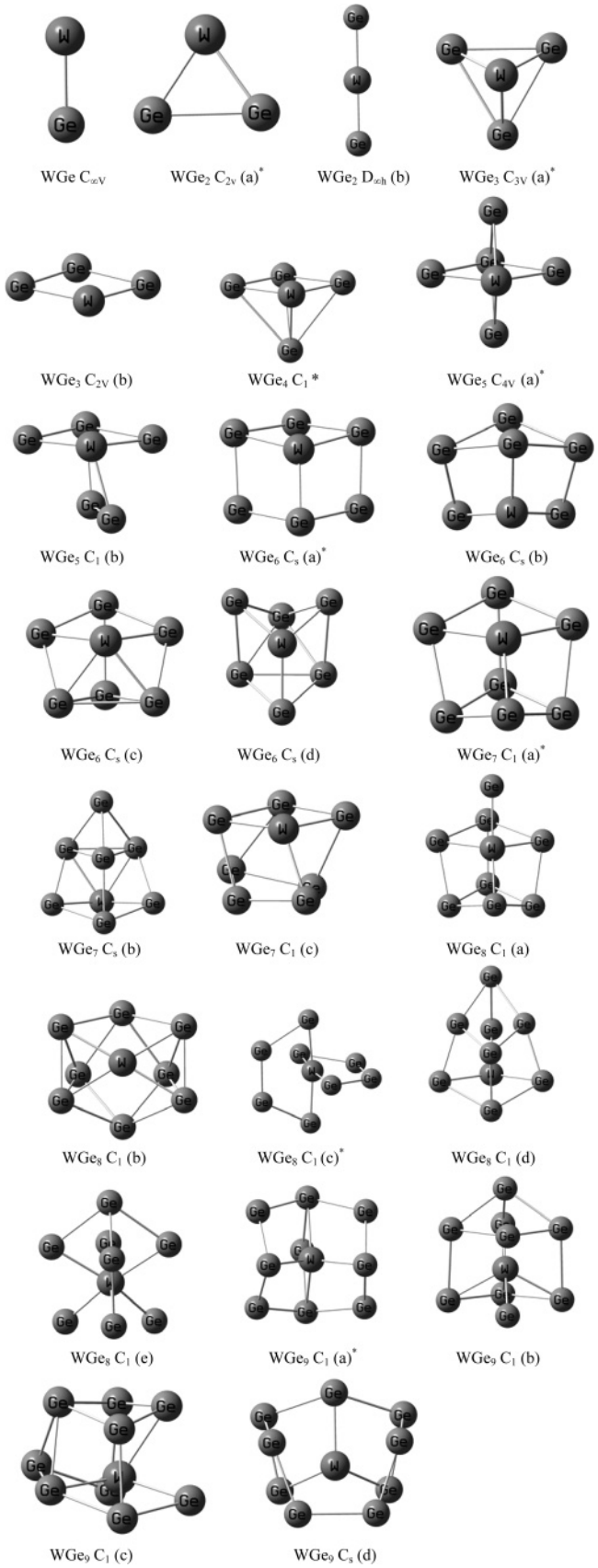

Figure 1. Equilibrium geometries of WGe_n (n = 1−9) clusters; asterisks indicate the lowest energy structures of all calculated minima.

optimized geometries of the examined systems, one finds that the WGe_{10} 10d isomer is the most stable isomer and the WGe_{10} 10d geometry is obviously different from that of the sandwich-like $ReSi_{10}$ isomer.[12] In analogy to the $OsGe_{10}$ cluster,[2] the sealed caged 10d structure is opened after geometry optimization, manifesting that the open caged structure is dominant for the W-doped germanium ($n = 10$) clusters, which are different from the first-row TM-doped Ge_{10} (TM = Cu, Ni, and Co) clusters.[4−6,13] In addition, the pentagonal prism sandwich-like 10b structure is found as a stable open caged structure after the insertion of the W atom into the caged Ge_{10} frame. However, its total energy is much higher than those of other identical sized isomers, reflecting that its stability is quite weakened as compared to that of the other identical sized isomers.

As far as the WGe_{11} clusters are concerned, the most stable 11a isomer is yielded after the 11th Ge atom, which causes the distortion of the 11a geometry and eliminates the dangling bonds of the germanium atoms, is capped on the bicapped tetragonal antiprism WGe_{10} 10d geometry. Two stable 11b and 11c structures are generated by aid of the different Ge surface-capped atoms on the pentagonal prism of the 10d isomer. The Ge face-capped pentagonal prism 10d is superior to the Ge edge-capped pentagonal prism 10d isomer in that the former is lower in total energy than the latter; therefore, the 11c is more stable than the 11b isomer.

Different from the first-row TM-doped Ge_{12} (TM = Cu and Ni) clusters,[4,13] a perfect hexagonal prism D_{3d} 12b isomer with W being encapsulated into a sealed caged Ge_{12} structure is generated, and its total energy is much lower than those of the other caged or basket-like TM-doped Ge_{12} structures. However, the other caged geometries with the W atom being not completely enclosed by germanium frames have some dangling bonds without being terminated by the enclosed W atom. Hence, the perfect hexagonal prism 12b structure has enhanced stability and is appropriate for the building block of quasi-one-dimensional W-doped germanium nanotubes. As seen from the examined equilibrium geometries of the WGe_n clusters, the identified structures for the most stable WGe_n are usually different from the $CuGe_n$, and $NiGe_n$ ($n = 1-12$) clusters; the two cluster series show different growth patterns in that the critical size for the $TMGe_n$ (TM = Co, Ni, and Cu) endohedral geometries was specified to be $n = 10$[4,13] while the critical size for the W atom being completely encapsulated into the caged germanium frame in the WGe_n clusters turns out to be $n = 12$. Interestingly, the encapsulated W atom in the 12b isomer, which is similar to the W in the WSi_{12} isomer,[3] tends to terminate the dangling bonds of the Ge atoms and behaves as an acceptor of charges, which is rooted in the tendency of W to attain a completely filled $5d^{10}$ configuration. In addition, for the first-row TM-doped Ge_{12} (TM = Cu and Ni), the basket-like structures are the lowest energy structures;[4,13] For the WGe_{12} cluster, however, the stability of the irregular basket-like 12f structure is quite weakened as compared to that of the hexagonal prism 12b isomer because of the 12f isomer being higher in total energy than the 12b isomer. On the basis of the calculated $TMGe_n$ (M = W, Ni, Cu, and Co; $n = 1-12$)[4,13] geometries, one concludes that the growth path of the $TMGe_n$ clusters strongly depends on the nature of the TM impurity and that the growth behaviors of the W-doped Ge_n clusters are obviously different from those of the TM-doped Ge_n (TM = Ni, Cu, and Co) clusters.[4,13]

The stable WGe_{13} 13a geometry is yielded after the 13th Ge atom is capped on the hexagonal prism WGe_{12} 12b geometry. As compared to other stable structures, the 13a is the most stable isomer because its total energy is the lowest one in all stable isomers. As shown in Figure 2, the tricapped pentagonal prism 13b and 13c isomers are emerged by capping germanium atoms on pentagonal prism WGe_{10} 10b and bicapped tetragonal antiprism 10d isomers, respectively. One finds that the 13b and 13c isomers are the open caged structures, the W atom is not totally enclosed by the germanium cage, and some dangling bonds of germanium atoms exist as compared to the 13a isomer. For example, the distance between the fourth and 13th germanium atoms in the 13b isomer is approximately 3.41 Å; both the fourth and 13th Ge atoms are simultaneously bonded with the W atom with equivalent bond lengths of 2.55 Å, and the open cagelike structure is formed finally. The 13b and 13c isomers are less stable than the 13a isomer because the coordinated germanium atoms of the W atom in the former are bigger than those of the latter. Hence, the stability of the W-encapsulated caged Ge_n clusters is related with the number of germanium atoms coordinated with the W atom. It should be pointed out that the basket-like 13e structure with the W atom being doped in the basket-like pure Ge_{13} cluster is seriously distorted after geometry optimization; however, the previous investigation on the Cu-doped basket-like Ge_n structures indicates that the basket-like geometry is not obviously distorted when the Cu atom is trapped into the basket-like germanium cage.[13]

With respect to the WGe_{14} equilibrium geometries, all optimized WGe_{14} structures are shown as the W-encapsulated sealed Ge_{14} cage. The most stable fullerene-like WGe_{14} 14a isomer, which is composed of six pentagons and three rhombi, is generated. A low-lying 14b isomer, which is generated from the WGe_{13} 13b isomer, can be found as a stable structure, and its total energy is higher than that of the 14a isomer by 0.46 eV. As shown in Figure 2, when one Ge atom is capped between the fourth and 13th Ge atoms of the WGe_{13} 13b isomer, a sealed caged 14b WGe_{14} cluster is obtained. Another stable 14c isomer with total energy being much close to the 14b isomer can be described as the tetracapped pentagonal prism and it is slightly different from the 14b isomer in that the Ge−Ge dimer symmetrically distributes at each side of pentagonal prism. Additionally, two kinds of pyramidal 14d and 14e structures are found as the stable structures; however, their total energies are higher than those of other isomers.

The WGe_{15} 15b structure, which keeps the framework that is analogous to the fullerene-like WGe_{14} isomer being proven to be a special stable structure, is a low-lying isomer. According to the calculated total energy, it is shown that the basket-like or pyramidal structures are lower in total energies than the fullerene-like structure, e.g., the total energy of the most stable 15d structure is lower than that of the 15b isomer by 0.26 eV. Except for the stable WGe_{15} clusters mentioned above, some low-lying amorphous 15e and 15f isomers are also considered and optimized; the low-lying 15e isomer is yielded after the extra germanium atoms are capped on the hexagonal prism12b isomer, and its total energy is much higher than that of the most stable 15d isomer by 1.36 eV. Consequently, the 15d isomer is selected as the most stable isomer and ground state.

For the WGe_{16} clusters, the most stable fullerene-like 16a isomer, the amorphous low-lying 16b and 16c isomers are considered and optimized. It should be mentioned that the fullerene-like WGe_{16} 16a geometry with unbalanced Ge bonds is different from that of the $TM@Si_{16}$ isomers.[16,17] Additionally, another 16b isomer, which is obtained after the Ge atoms are capped on the pentagonal prism 12b isomer, is much higher in

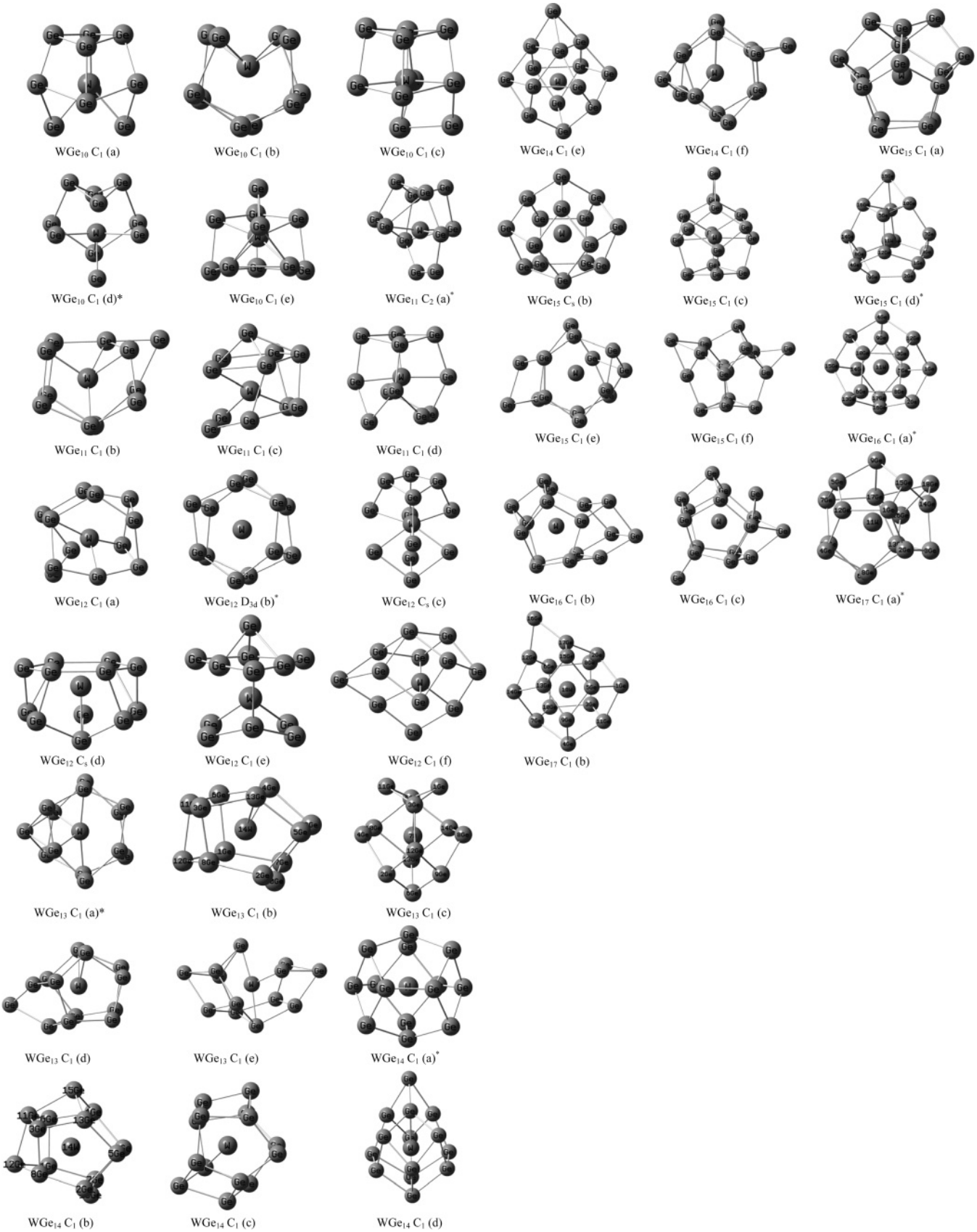

Figure 2. Equilibrium geometries of WGe_n ($n = 10-17$) structures; asterisks indicate the lowest energy structures of all calculated minima.

total energy as compared to the fullerene-like 16a structure. However, in case of the WGe_{17} clusters, the amorphous 17a isomer, which is obtained from the Ge-capped pentagonal prism 12b isomer, is lower in total energy than the 17b isomer which is obtained from the fullerene-like WGe_{16} 16a cluster.

In summary, the W-encapsulated sealed caged germanium clusters are emerged as $n = 12$; the critical size with W being completely enclosed in Ge_n frames is larger than that of the first-row TM-encapsulated sealed caged germanium clusters (TM = Ni and Cu; $n = 10$). Different from the first-row TM-

doped germanium clusters (TM = Ni and Cu), the hexagonal prism-like WGe_n structures are distinctly lower in total energies than the basket-like WGe_n structures. Moreover, the W-encapsulated fullerene-like WGe_n structure first emerges as $n = 14$ and has special stability as compared to the basket-like or pyramidal WGe_n structures; However, the basket-like or pyramidal WGe_{15} 15d cluster, which can be seen as the exception, is stronger in stability than the fullerene-like WGe_{15} 15b structure. Different from the $TM@Si_{16}$ clusters,[16,17] the fullerene-like $W@Ge_{16}$ structure has unequivalent bond lengths among the W and all the germanium atoms and has the same coordinated number as those of the $TM@Si_{16}$ clusters;[16,17] furthermore, the calculated results on the $W@Ge_{16}$ structure show that the W atom in the $W@Ge_{16}$ interacts with the p_z orbitals of all Ge atoms with covalent bonds and that the covalent bonds among the p_z orbitals of each Ge atom and the enclosed W atom result in the strong stability of this cluster.

III.C. Relative Stability of Different-Sized W-Doped Germanium Clusters. It is important to obtain and discuss the relative stability of different sized clusters because the special species can act as the building block of novel optoelectronic nanomaterials. The relative stability of different sized WGe_n clusters can be reflected from the averaged atomic binding energies and fragmentation energies. The averaged atomic binding energies and fragmentation energies of the WGe_n clusters can be described by the following formula:

$$E_b(n) = [E_T(W) + nE_T(Ge) - E_T(WGe_n)]/n + 1$$

$$D(n, n-1) = E_T(WGe_{n-1}) + E_T(Ge) - E_T(WGe_n)$$

where $E_T(WGe_{n-1})$, $E_T(Ge)$, $E_T(W)$, and $E_T(WGe_n)$ represent the total energies of the lowest energy WGe_{n-1}, Ge, W, and WGe_n clusters, respectively.

The calculated results of the averaged atomic binding energies are plotted as the curves which show sized dependence of the averaged atomic binding energies of WGe_n clusters; The third-row W-doped pure germanium clusters pertaining to the averaged atomic binding energy are larger than those of the first-row $TMGe_n$ (TM = Cu and Ni) clusters. Additionally, the investigated TM-doped Ge_n (TM = W, Co, Cu, and Ni)[4,13] clusters and pure Ge_n clusters indicate that different transition metal doped germanium clusters have different influences to the averaged atomic binding energies of pure germanium clusters (Figure 3).

On the other hand, the calculated fragmentation energies of different sized WGe_n clusters can give the information of relative stabilities of clusters and provide the most stable building block of cluster-assembled materials. As shown in Figure 4, the local maxima of $D(n, n-1)$ of WGe_n clusters localize at 5, 8, 12, 14, and 16, respectively, which are obviously different from those of the first-row TM-doped germanium clusters (TM = Cu and Ni). Previous experimental and theoretical results indicated that the first-row TM (TM = Cu and Ni) doped Ge_{10} clusters have the strongest stability and the lowest energy TM-encapsulated symmetrical bicapped tetragonal antiprism rhombi, which corresponds to enhanced abundances observed for these species by mass spectroscopy.[1,4−6] However, the Ge_{10} frame of the WGe_{10} geometry is changed from the seal caged structure to the open caged structure after the W atom is doped into the Ge_{10} cage. Although the bicapped tetragonal antiprism rhombi WGe_{10} 10d is optimized as the lowest energy structure in all stable isomers, the geometry is obviously an open caged structure and has some dangling bonds that affect the stabilities of clusters. Different from the first-row TM-doped Ge_{12} (TM = Cu and Ni) clusters,[4,13] the stability of the hexagonal prism WGe_{12} cluster is evidently increased and is apparently stronger than those of the adjacent sized clusters. As compared to the hexagonal prism $TM@Ge_{12}$ (TM = Cu and Ni) structure,[4,13] the hexagonal prism WGe_{12} cluster is a sealed caged D_{3d} structure. Except for the typical bicapped tetragonal antiprism WGe_{10} and hexagonal prism WGe_{12} isomers, the relative stabilities of the larger-sized clusters are also investigated in this work. The calculated relative stabilities of fullerene-like WGe_{14} or WGe_{16} structures are stronger than that of the basket-like or pyramidal WGe_{15} structure because the enclosed W atom in the Ge_{14} and Ge_{16} frames interacts with all germanium atoms with coordinated numbers of 14 and 16, respectively. In addition, the fullerene-like WGe_{14} isomer is the 18-electron rule system with a full closed electron configuration. On the basis of the above discussions, it is indicated that the large-sized WGe_n clusters exhibit special geometric and electronic characteristics as well as the relative stabilities which differ from those of the $TMSi_n$[16,17] and $TMGe_n$ (TM = Cu, Co, and Ni) clusters.[4,13]

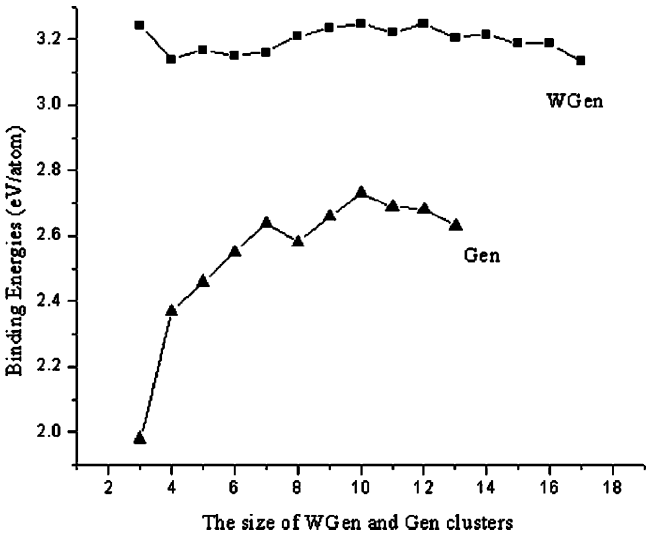

Figure 3. Sized dependence of the averaged atomic binding energies of WGe_n ($n = 3-17$) and pure Ge_n ($n = 3-13$) clusters.

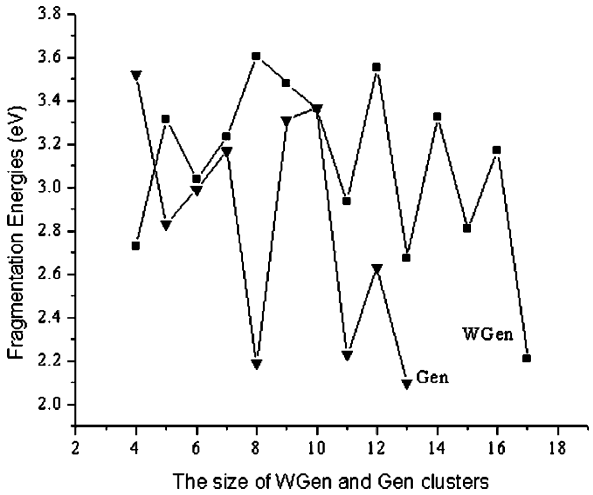

Figure 4. Sized dependence of fragmentation energies of WGe_n ($n = 4-17$) and pure Ge_n ($n = 4-13$) clusters.

III.D. HOMO−LUMO Gap. It is useful to study the HOMO−LUMO gaps because the closed electronic configuration with a large HOMO−LUMO gap is necessary for the chemical stability of a cluster. As illustrated in Table 3, the HOMO−LUMO gap of the large-sized fullerene-like cluster is

TABLE 3: Natural Charge Population, HOMO−LUMO Gap, and Dipole Moment of the Located Lowest Energy Structures with Spin Singlet State of Different Sized WGe_n (n = 3−17) Clusters

cluster	natural population	HOMO−LUMO gap (eV)	dipole moment (D)
WGe_3	−0.893	3.058	2.455
WGe_4	−0.771	2.46	2.375
WGe_5	−0.663	2.707	2.619
WGe_6	−0.739	2.374	1.679
WGe_7	−0.795	2.328	2.013
WGe_8	−2.248	2.519	0.082
WGe_9	−1.813	2.53	0.066
WGe_{10}	−2.349	2.454	1.418
WGe_{11}	−2.072	2.652	0.128
WGe_{12}	−1.625	2.334	0
WGe_{13}	−1.774	2.364	0.578
WGe_{14}	−1.973	1.852	0.027
WGe_{15}	−1.964	1.512	1.134
WGe_{16}	−1.783	1.816	0.684
WGe_{17}	−1.782	1.463	0.389

smaller than that of the small-sized cluster. It should be mentioned that the HOMO−LUMO gap of the fullerene-like WGe_{16} is smaller than that of $Zr@Si_{16}$[17] and the WGe_{16} is not of the same stability as $Zr@Si_{16}$ in the dissociation. Additionally, the HOMO−LUMO gap (2.334 eV) of the hexagonal prism WGe_{12} is distinctly increased as compared to that of the pure Ge_{12} (1.705 eV) or $NiGe_{12}$ (1.691 eV) clusters.[4,13] Hence, the neutral symmetrical hexagonal prism WGe_{12} cluster with a large HOMO−LUMO gap, large fragmentation energy, and large averaged atomic binding energy is suitable as the new building block of assembly cluster material because of its strong chemical stability. This finding is distinctly different from those of the first-row $TM@Ge_{10}$ (TM = Cu and Ni) isomers. The third-row heavy W-doped germanium cluster has a specially stable WGe_{12} unit which is similar to the $W@Si_{12}$ cluster,[3,18,19] reflecting that stability of the pure germanium cluster is obviously strengthened when the heavy W atom is enclosed in its Ge_n frames.

III.E. Charge-Transfer Mechanism and Polarity. It is valuable to investigate the charge-transfer mechanism of the TM-doped caged germanium clusters because the hybrid sp^3 germanium atoms tends to make germanium chains being three-dimensional structures and is not superior to forming quasi-one-dimensional nanotubes. Only the charge-transfer of the TM-doped germanium cluster makes it possible to form sp^2 germanium atoms and plays an important role in forming nanowires of germanium clusters. As illustrated in Table 3, charges in the WGe_n clusters transfer from the germanium framework to the W atom, indicating that the W atom easily accepts electrons from the germanium framework which is related to the degree of 5d shell saturation of the W atom. In addition, the negative charges of the W atom in the caged clusters (n > 7) are bigger than those of the W atom in the small-sized clusters (n < 7), reflecting that the W accepts abundant electrons from the germanium cages and forms hybrid sp^2 germanium atoms. Interestingly, the W-doped germanium clusters have different charge-transfer phenomena as compared to the first-row TM-doped germanium (TM = Cu and Ni) clusters[4,13] because the charges in the $CuGe_n$ clusters always transfer from the Cu atom to the germanium atoms,[13] while the charges in the $NiGe_n$ (n < 6 and n > 11) clusters transfer from the Ni atom to the Ge_n atoms and charges in the middle- or large-sized $NiGe_n$ (n > 6) clusters transfer from the Ge_n atoms to the Ni atom.[4] These results again indicate that the heavy W atom is beneficial for eliminating excess electrons in the germanium framework and contributes to forming a hybrid sp^2 germanium cage as compared to the first-row TM-doped Ge_n (TM = Cu and Ni) clusters.

Previous investigations on the bicapped tetragonal antiprism $TM@Ge_{10}$ (TM = Cu and Ni) clusters indicate that their dipole moments are very small[4,13] because the optimized $TM@Ge_{10}$ (TM = Cu and Ni) geometries have higher symmetries and almost equivalent bond lengths between the TM and germanium atoms. On the contrary, the bicapped tetragonal antiprism WGe_{10} has obvious polarity and its dipole moment is 1.418 D in that the bicapped tetragonal antiprism WGe_{10} geometry is significantly distorted and has obviously different W−Ge bond lengths and an unsymmetrical distribution of germanium atoms around the W atom which give rise to the polarity. As for the hexagonal prism $NiGe_{12}$ and $ZrSi_{12}$ clusters with the dipole moment being, respectively, 0.796 and 1.022 D, they are obviously the polar molecules;[17] on the contrary, the dipole moment of the hexagonal prism WGe_{12} is 0 D, corresponding to a nonpolar cluster with D_{3d} symmetry.

In addition, the fullerene-like $ZrSi_{16}$ cluster with the dipole moment of 0.022 D is nearly a nonpolar cluster[17] because all silicon atoms in the $ZrSi_{16}$ are symmetrically distributed around the Zr atom. However, the WGe_{16} has obvious polarity with the dipole moment being 0.684 D, and the germanium atoms around the W in the WGe_{16} are not symmetrically distributed except for one Ge atom being far away from the W atom as compared to the other germanium atoms. Hence, the distribution of the germanium atoms around the transition metal W atom in the WGe_{16} cluster affects the polarity and the relative stability of the clusters.

IV. Conclusion

Equilibrium geometries, stabilities, energy gaps, and polarities of the tungsten-doped germanium clusters (n = 1−17) are systematically investigated using the (U)B3LYP/LanL2DZ method. All the results are summarized as follows:

(1) The threshold size of the caged WGe_n clusters and the critical size of the sealed W-encapsulated Ge_n structure emerge at, respectively, n = 8 and n = 12, and the remarkable WGe_{14} geometry is a fullerene-like structure. These findings, however, differ from those of the first-row TM-doped germanium clusters (TM = Cu and Ni) with the critical size of the sealed TM-encapsulated structures appearing at n = 10. Hence, the large differences of the equilibrium geometries between the first-row TM-doped (TM = Cu and Ni) germanium clusters and the third-row W-doped caged germanium clusters indicate the different growth behaviors. In other words, the growth patterns are dependent on the doped transition metals.

(2) The calculated results show that the relative stability of the hexagonal prism $TM@Ge_{12}$ (TM = Cu and Ni) is weaker than that of the basket-like $TM@Ge_{12}$ (TM = Cu and Ni) structures. On the contrary, the stability of the lowest energy hexagonal prism WGe_{12} is obviously increased as compared to that of the basket-like WGe_n structures. The magic numbers of relative stabilities in terms of the calculated fragmentation energies are, respectively, 5, 8, 12, 14, and 16. It should be mentioned that the relative stability of the bicapped tetragonal antiprism WGe_{10} geometry is weakened as compared to that of its neighboring clusters, which differs apparently from those of the first-row $TM@Ge_{10}$ (TM = Cu, Ni, and Co) clusters.

(3) Different from the first-row TM-doped germanium (TM = Cu and Ni) clusters, charges always transfer from the Ge ligands to the tungsten atom at different sizes of clusters. This charge-transfer mechanism of the WGe_n clusters is beneficial

for the hybrid sp^2 germanium atoms and contributes to forming a fullerene-like structure.

(4) The HOMO−LUMO gap of the fullerene-like W-doped germanium clusters is obviously lower than those of the bicapped tetragonal antiprism WGe_{10} and the perfect hexagonal prism WGe_{12} clusters. The symmetrical hexagonal prism WGe_{12} cluster with a large HOMO−LUMO gap, large fragmentation energy, and large binding energy is suitable for the building block of assembly cluster material because of its strong chemical stability.

(5) Different from the bicapped tetragonal antiprism $TM@Ge_{10}$ (TM = Cu and Ni) and some fullerene-like $TM@Si_{16}$, the dipole moments of bicapped tetragonal antiprism WGe_{10} and fullerene-like WGe_{16} obviously exhibit that these species are the polar molecules. On the contrary, the dipole moment of hexagonal prism WGe_{12} is zero, corresponding to a nonpolar molecule.

Acknowledgment. This work is supported by the Natural Science Foundation of China (20173055). H.J.-G. thanks Dr. Run-Ning Zhao (Northwestern University, Xi'an, Shanxi 710069) for her useful discussions and help.

References and Notes

(1) Zhang, X.; Li, G. L.; Gao, Z. *Rapid Commun. Mass Spectrom.* **2001**, *15*, 1573.

(2) Lu, J.; Nagase, S. *Chem. Phys. Lett.* **2003**, *372*, 394.

(3) Han, J. G.; Xiao, C. Y.; Hagelberg, F. *Struct. Chem.* **2002**, *13*, 173.

(4) Wang, J.; Han, J. G. *J. Phys. Chem. B* **2006**, *110*, 7820.

(5) Li, G. L.; Zhang, X.; Tang, Z.; Gao, Z. *Chem. Phys. Lett.* **2002**, *359*, 203.

(6) Kumar, V.; Singh, A. K.; Kawazoe, Y. *Nano Lett.* **2004**, *4*, 677.

(7) Wadt, W. R.; Hay, P. J. *J. Chem. Phys.* **1985**, *82*, 284.

(8) (a) Becke, A. D. *Phys. Rev. A* **1998**, *38*, 3098. (b) Lee, C.; Yang, W.; Parr, R. G. *Phys. Rev. B* **1998**, *27*, 785.

(9) Guo, P.; Ren, Z. Y.; Wang, F.; Bian, J.; Han, J. G.; Wang, G. H. *J. Chem. Phys*. **2004**, *121*, 12265.

(10) Han, J. G.; Hagelberg, F. *Chem. Phys*. **2001**, *263*, 255.

(11) Han, J. G. *Chem. Phys*. **2003**, *286*, 181.

(12) Han, J. G.; Ren, Z. Y.; Lu, B. Z. *J. Phys. Chem. A* **2004**, *108*, 5100.

(13) Wang, J.; Han, J. G. *J. Chem. Phys.* **2005**, *123*, 64306.

(14) (a) Hu, Z. D.; Dong, J. G.; Lombardi, J. R.; Lindsay, D. M. *J. Chem. Phys*. **1992**, *97*, 9811. (b) Wu, Z. J. *Chem. Phys. Lett.* **2003**, *370*, 510.

(15) Frisch, M. J.; Trucks, G. W.; Schlegel, H. B.; Scuseria, G. E.; Robb, M. A.; Cheeseman, J. R.; Montgomery, J. A., Jr.; Vreven, T.; Kudin, K. N.; Burant, J. C.; Millam, J. M.; Iyengar, S. S.; Tomasi, J.; Barone, V.; Mennucci, B.; Cossi, M.; Scalmani, G.; Rega, N.; Petersson, G. A.; Nakatsuji, H.; Hada, M.; Ehara, M.; Toyota, K.; Fukuda, R.; Hasegawa, J.; Ishida, M.; Nakajima, T.; Honda, Y.; Kitao, O.; Nakai, H.; Klene, M.; Li, X.; Knox, J. E.; Hratchian, H. P.; Cross, J. B.; Bakken, V.; Adamo, C.; Jaramillo, J.; Gomperts, R.; Stratmann, R. E.; Yazyev, O.; Austin, A. J.; Cammi, R.; Pomelli, C.; Ochterski, J. W.; Ayala, P. Y.; Morokuma, K.; Voth, G. A.; Salvador, P.; Dannenberg, J. J.; Zakrzewski, V. G.; Dapprich, S.; Daniels, A. D.; Strain, M. C.; Farkas, O.; Malick, D. K.; Rabuck, A. D.; Raghavachari, K.; Foresman, J. B.; Ortiz, J. V.; Cui, Q.; Baboul, A. G.; Clifford, S.; Cioslowski, J.; Stefanov, B. B.; Liu, G.; Liashenko, A.; Piskorz, P.; Komaromi, I.; Martin, R. L.; Fox, D. J.; Keith, T.; Al-Laham, M. A.; Peng, C. Y.; Nanayakkara, A.; Challacombe, M.; Gill, P. M. W.; Johnson, B.; Chen, W.; Wong, M. W.; Gonzalez, C.; Pople, J. A. *Gaussian03*; Gaussian, Inc.: Wallingford, CT, 2004.

(16) Kumar, V.; Kawazoe, Y. *Phys. Rev. Lett.* **2001**, *87*, 045503.

(17) Wang, J.; Han, J. G. *J. Chem. Phys.* **2005**, *123*, 64306.

(18) Lu, J.; Nagase, S. *Phys. Rev. Lett.* **2003**, *90*, 115506.

(19) Hiura, H.; Miyazaki, T.; Kanayama, T. *Phys. Rev. Lett*. **2001**, *86*, 1733.